



A PROTOTYPE RING-IMAGING WATER CERENKOV DETECTOR
FOR NEUTRINO-ELECTRON SCATTERING

P. Bloch³(*), A. Blondel², J.M. Candelle³, J. Feltesse³,
R. Fries²(**), C. Gregory², F. Jacquet², R. Legac²,
A. Milsztajn³, A. Staude¹, M. Virchaux³ and R. Voss¹

ABSTRACT

A small scale prototype of a Cerenkov detector to study ν_e scattering using water as an active target has been constructed and tested with electron, muon, photon, and pion beams. We find an angular resolution for electrons of $6 \text{ mrad}/\sqrt{E[\text{GeV}]}$ and good discrimination between electrons, photons, and hadrons.

Submitted to Nuclear Instruments and Methods in Physics Research

1 Sektion Physik der Universität, Munich, Federal Republic of Germany

2 Ecole Polytechnique, Palaiseau, France

3 CEN, Saclay, France

(*) Now at CERN

(**) Now at Bundesministerium für Wissenschaft und Forschung, Wien, Austria.

1. INTRODUCTION

The purely leptonic neutral current reaction $\nu_{\mu} e \rightarrow \nu_{\mu} e$ is well suited for a precise determination of the electroweak mixing angle θ_W in the low Q^2 regime. The ratio of the cross sections $\frac{d\sigma}{dy}(\nu_{\mu} e^{-}) / \frac{d\sigma}{dy}(\bar{\nu}_{\mu} e^{-})$ is very sensitive to $\sin^2\theta_W$, and the sensitivity increases with $y = E_e/E_{\nu}$, the relative energy transfer to the electron.

Because of the low mass of the target electron, neutrino-electron scattering has two significant characteristics. The angle of the scattered electron with respect to the neutrino is very small ($\theta_e = \sqrt{(2m_e/E_e)(1-y)} \ll 32 \text{ mrad}/\sqrt{E[\text{GeV}]}$), and the cross section is about 10^4 times smaller than the cross section for neutrino-nucleon interactions.

A detector for ν - e scattering should therefore have a good angular resolution to measure the y distribution, combined with a large detection mass. Also, a good particle identification is needed to separate electrons from hadron and photon background.

We have studied a novel detector [1] which uses a large water volume as target and measures the Cerenkov light cone emitted by the charged tracks. Here, we report results from a test of a prototype exposed to electron, muon, pion and gamma beams.

2. THE EXPERIMENTAL SET-UP

2.1 The Detection Principle

The apparatus exploits the following two detection principles:

- (a) Fast charged particles in water produce a Cerenkov light cone of 42° half opening angle. If the particle direction is inclined upwards with respect to the water surface, a section of the light cone leaves the water [2] and is focused by a spherical mirror on a detector plane. Neglecting optical distortions, the image produced in the focal plane is an arc of a circle (Fig. 1). The position of this arc depends only

on the direction of the particle. Therefore, the image of a straight track traversing the water volume is a single arc in the focal plane whereas showering particles give a superposition of arcs which reflect the angular distribution of the shower particles.

- (b) Electrons and γ -rays give identical patterns in the focal plane but can be distinguished in the initial development phase of the shower from the different number of Cerenkov photons emitted along the first fraction of a radiation length. The shower subsequently develops into a large number of wide angle tracks producing a halo of Cerenkov light which deteriorates the information about the beginning of the track unless it is suppressed experimentally. The measurement of the longitudinal shower development is therefore restricted to light from particles produced within a small (≈ 100 mrad) cone around the beam direction.

2.2 The Test Set-up (Fig. 2)

The beam traversed a water tank 1.5 m high, 1 m wide and 4.5 m long with an upwards inclination of 42 mrad to simulate the CERN neutrino beam. The demineralized water had an initial absorption length of 5 m for photons of $\lambda = 450$ nm; since the water was not continuously purified, this degraded to about 2 m during the 6 weeks data taking time. For most of the measurements, a 4 mm thick glass plate covered the water surface in order to suppress surface waves caused by a nearby operating bubble chamber.

The spherical mirror was installed above the downstream end of the tank and had a focal length of 6 m. It was 60 cm wide and 180 cm high; the optical quality was better than 0.1 mrad. An array of 105 photomultipliers (PMs) of 2" diameter (EMI 98142 KB) covered an area of 90 x 90 cm² in the focal plane (forward detector). Conical reflectors increased the sensitive area covered by each tube to ≈ 57 cm². Each PM was connected to an integrating high resolution ADC. The light leaves the water close to the angle of total reflection which causes a change of the vertical angle to be amplified by a factor 3.5 by the refraction. In addition, since this set-up detects only a small azimuthal section of the Cerenkov light cone

(± 65 mrad with respect to the vertical axis), the position of the image in the focal plane is almost insensitive to the horizontal angle of the particle and only the vertical component of the particle direction is measured. The measurement is geometrically limited to ± 20 mrad with respect to the beam axis by the size of the focal plane detector.

The gain of the focal plane PM's was equalized, and monitored in regular intervals, by illuminating the focal plane with four light diodes. The conversion of measured pulse height to photoelectrons was determined both from the relative width of the pulse height distribution for LED signals and directly from the single photoelectron response of the PMs, measured with very weak LED pulses. Both methods gave results compatible to within $\pm 10\%$.

In order to study the longitudinal shower development, 48 phototubes (RTC XP2330) are arranged in eight columns of three tubes each on both sides of the tank. The phototubes are oriented towards the Cerenkov light but view the water through an arrangement of glass plates forming an air wedge between the water and the cathodes of the phototubes (Fig. 2b). They are sensitive only to Cerenkov photons emitted by shower particles at small angles with respect to the beam direction (≈ 100 mrad). Each of the columns of this "shower scanner" views 12 cm - corresponding to $1/3$ of a radiation length (X_0) - of the trajectory along the beam axis, with the exception of the first two ones. The first column observes only back-scattered light and the second only the first 9 cm inside the tank. The response of the tubes was normalized using muon-tracks; we observe about three photoelectrons per PM per 12 cm of minimum ionizing track.

The test was performed in the X5 beam at the CERN SPS which allows for negative charged particles only; trigger counters immediately in front of our detector limited the beam dimensions to 2×2 cm². We recorded data at beam momenta between 3 and 30 GeV/c. Muons were tagged with a shielded counter placed behind the detector. In order to distinguish pions from lighter particles, we used a signal from two helium filled Cerenkov counters upstream in the beam line. We also set up a tagged photon beam covering an energy range between 5 and 20 GeV. For triggering purposes, the photons were converted in a thin lead foil in front of the detector.

3. ANGULAR MEASUREMENT

As mentioned above, the Cerenkov photons emitted by a straight track are focussed on an arc of circle. Fig. 3a shows the responses of the photomultipliers in the focal plane for a single muon. The signal of each phototube is represented by the surface of a small disc.

The hit phototubes cluster clearly along the arc corresponding to the beam angle (42 mrad) with almost no background. Fig. 3b shows the projection of the PM signals in bins of θ_z . These bins are smaller than the angular range covered by one PM. Therefore, each PM signal is distributed over several bins with weights proportional to the overlap of the focal plane area covered by the PM reflectors and the respective θ_z bin. The width of this distribution, which we call the θ ideogram, is mainly due to the finite size of the reflectors.

The reconstructed angle of the muon is defined as the position of the maximum in this θ ideogram. With this definition, the resolution $\sigma(\theta_z)$ obtained for 30 GeV muon tracks is ≈ 1 mrad, compatible with beam divergence and multiple scattering in the water.

For electrons, the ring image is smeared due to multiple scattering of the shower particles. However, the shower retains the direction of the primary electron as shown by the display of a single electron event (fig. 4). It is therefore still valid to define the electron angle as the position of the θ -ideogram maxima. This simple method of reconstruction is, however, sensitive to statistical fluctuations of individual PMs. In order to minimize this effect we use a more refined method: We first define the typical shape of the photon angular distribution by averaging many electron events at a given angle θ_0 ; from this, we obtain a curve $f(\theta-\theta_0)$ peaked at this angle θ_0 . The angle of each individual event is then obtained by a fit of this distribution to the data with θ_0 as the only free parameter. We have checked that the results are insensitive to the exact shape of the fitted angular distribution. Fig. 5 shows the distribution of angles reconstructed with both methods for 5 and 15 GeV electrons. Measurements made at different beam angles show that the results are also insensitive, within our acceptance, to the position of the mean angle.

Since the resolution curves do not behave gaussian, we characterize them by their $\sigma = \text{FWHM}/2.3$ and by the fraction of events lying outside $\pm 2\sigma$ (fig 6). This σ follows approximately a law $\sigma = 6 \text{ mrad}\sqrt{E[\text{GeV}]}$.

4. ELECTRON IDENTIFICATION

4.1 Electron-Hadron separation

For electrons, the total light intensity measured in the focal plane is proportional to the electron energy. The energy resolution computed from the r.m.s. width of this intensity distribution is $\sigma(E)/E = 30\%/\sqrt{E[\text{GeV}]}$.

The light intensity from pions is drastically different (Fig.7). This feature can be used to discriminate between electrons and hadrons if the energy of the particle is known^(*). A pion rejection by a factor 100 can be achieved with an efficiency of 97% for electrons.

Since the longitudinal development of the shower is also different for electrons and pions, the shower scanner can be used to improve the e/π rejection by a factor 10 as shown in Fig. 8.

Using these results in the simulation of the ν_μ -e experiment [1], taking into account the angular and energy distribution of the hadrons produced in the neutrino interaction, we arrive at a rejection of ν -nucleon interactions which is better than 10^5 .

(*) The energy of the particle could, for example, be measured by sampling the emitted Cerenkov light over the total surface of the water tank without angular selection, as it is done in the IMB proton lifetime experiment [4].

4.2 Electron-photon separation

The shower scanner measures the longitudinal shower development along the first 3 radiation lengths. For the study of $e\text{-}\gamma$ separation, we have compared a sample of 400 converted γ 's of 15 GeV energy to electrons of the same energy. The beginning of the shower is, on the average, clearly different for electrons and for photons.

As an example, Fig. 9 shows the pulse-height distributions in the first column sampling the shower along $1/4 X_0$, starting $1/12 X_0$ behind the conversion point. A selection on an event-by-event basis is achieved with appropriate cuts on the number of photoelectrons observed in the PM column viewing the origin of the shower.

In order to take into account the uncertainty on the conversion point when the water is used as converter, we have investigated the $e\text{-}\gamma$ separation at various distances from the shower origin (fig. 10). With a sampling every $1/3 X_0$, it is possible to retain 80% of the electrons with a γ rejection by a factor of 5.

4.3 Comparison with a Monte-Carlo simulation

We have compared our experimental results with a Monte-Carlo simulation, using the EGS program [3] with the addition of Cerenkov light emission. The exact geometry of the set-up is taken into account in the simulation.

The number of photoelectrons from muon tracks detected in the focal plane is 20 ± 2 per cm of track. Using this as an input to the EGS program, the Monte-Carlo simulation reproduces well the response of the focal plane detector to electrons.

We can also reproduce the signal in the shower scanner if we take into account that light detected in the focal plane is attenuated by:

- attenuation in water ($.73 \pm .02$)
- absorption in the window ($.78 \pm .05$)
- reflectivity of the collectors ($.83 \pm .05$)
- reflectivity of the spherical mirror ($.80 \pm .02$),

effects which do not exist or are less important for the shower scanner.

The photon angular distributions show a larger tail for data than for Monte-Carlo for both the muon and electron data. These tails can be reproduced by assuming diffusion of the Cerenkov photons in the water due to impurities.

5. CONCLUSIONS

This prototype test has shown the feasibility of a detector which uses water as an active target and measures, in complementary ways, the Cerenkov light emitted by the charged particles. Our detector has the following salient properties:

- (a) a very good angular resolution, about 3 times better than can be achieved with existing fine grain calorimeters but limited to a forward acceptance of ~ 100 mrad;
- (b) electron-photon separation by analysis of the early shower development;
- (c) excellent electron-hadron separation, obtained simply by comparing the light intensity measured in the focal plane to a total energy measurement. This can be used for a trigger to pick up rare forward electron or photon events.

To summarize, we believe that such a detector represents a genuine progress for measurements of rare single electron or photon events in the forward direction.

ACKNOWLEDGEMENTS

The support of D. Plane in setting up the beam and the detector has been indispensable for the success of this measurement, as well as the invaluable help of G. Bertalmio, H. Herbert, L. Kalt, M. Lemoine, B. Montes, E. Pasquetto and H. Willaredt. We also wish to thank M. Cuisenier from the Institut d'Astrophysique de Meudon for kindly making the spherical mirrors available to us.

REFERENCES

- [1] L. Behr et al., A proposal to measure ν_{μ} -e scattering with a large water Cerenkov detector, CERN/SPSC 84-31 (CERN/SPSC/P199), (unpublished).
- [2] J.W. Cronin and M.L. Swartz, Proposal to study neutrino-electron and antineutrino-electron scattering, Fermilab Proposal 600, 1978 (unpublished).
- [3] R.L. Ford and W.R. Nelson, SLAC-210 (1978).
- [4] R.M. Bionta, Proc. 19th Rencontre de Moriond, La Plagne, Savoie, France, J. Tran Thanh Van ed., Vol. 1, p. 611 (1984).

FIGURE CAPTIONS

- Fig. 1 Principle of the forward detector.
- Fig. 2a) Layout of the test set-up;
2b) Detail of a shower scanner unit.
- Fig. 3a) Focal plane display of a 30 GeV muon track. The dashed lines correspond to fixed vertical angles θ_z of tracks in water.
3b) θ_z ideogram of the same event (see text).
- Fig. 4 As fig. 3 for a 15 GeV electron.
- Fig. 5 Angular distribution of 5 and 15 GeV electrons:
5a) obtained from the maxima of the θ_z ideogram;
5b) obtained from fits to the PM pulse height distribution.
- Fig. 6 Angular resolution of the forward detector and fraction of events outside a 2σ cut as function of the electron energy σ is calculated as $\text{FWHM}/2.35$.
- Fig. 7 Total pulse height in the focal plane for 10 GeV electrons and pions.
- Fig. 8 Scatter plot of total pulse height in the focal plane vs. total pulse height in the shower scanner for electrons and pions. The lines indicate the cut used to separate electrons and pions.
- Fig. 9 Pulse height distribution of the second shower scanner column for electrons and photons.
- Fig. 10 $e\text{-}\gamma$ separation using the pulse height from single shower scanner columns only.

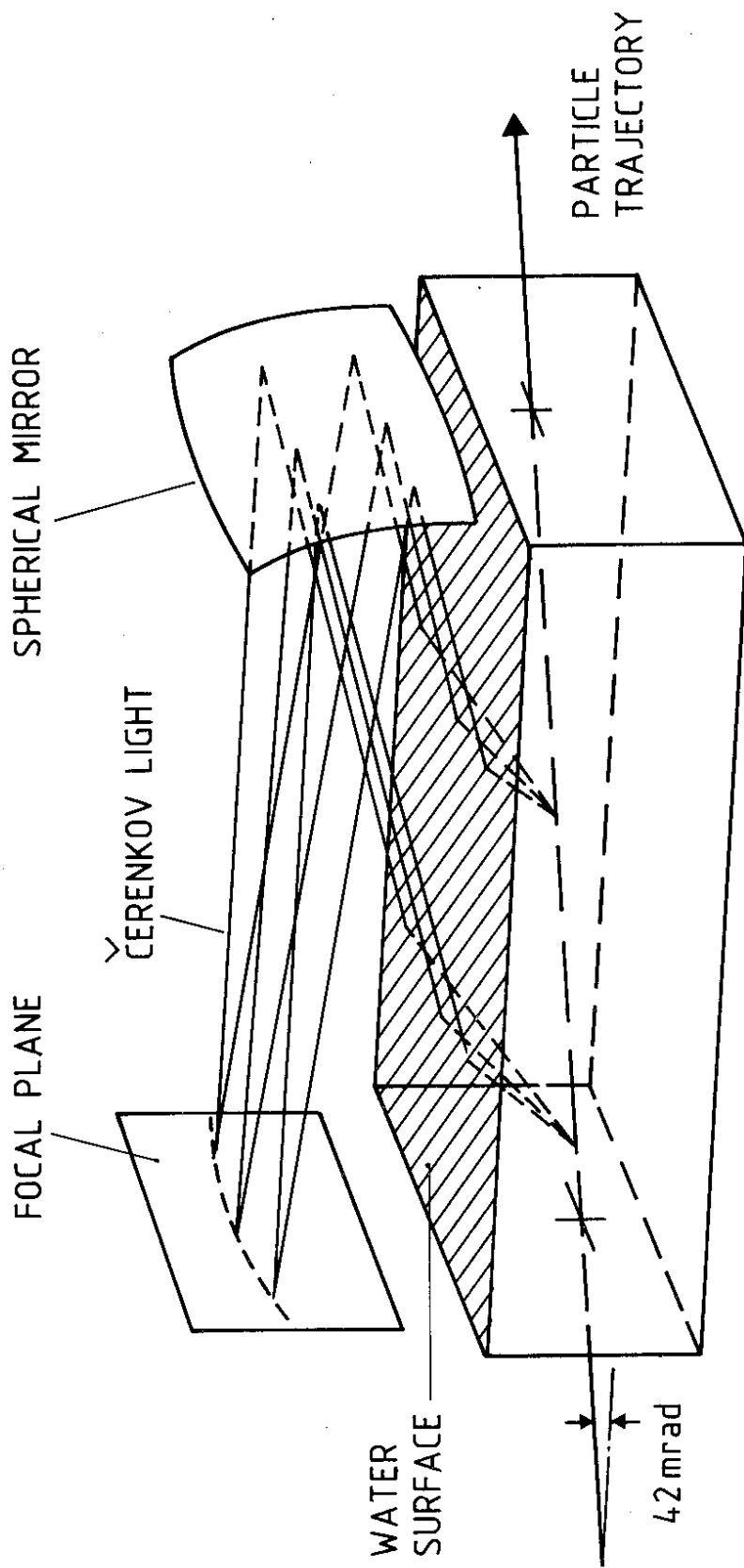


FIG. 1

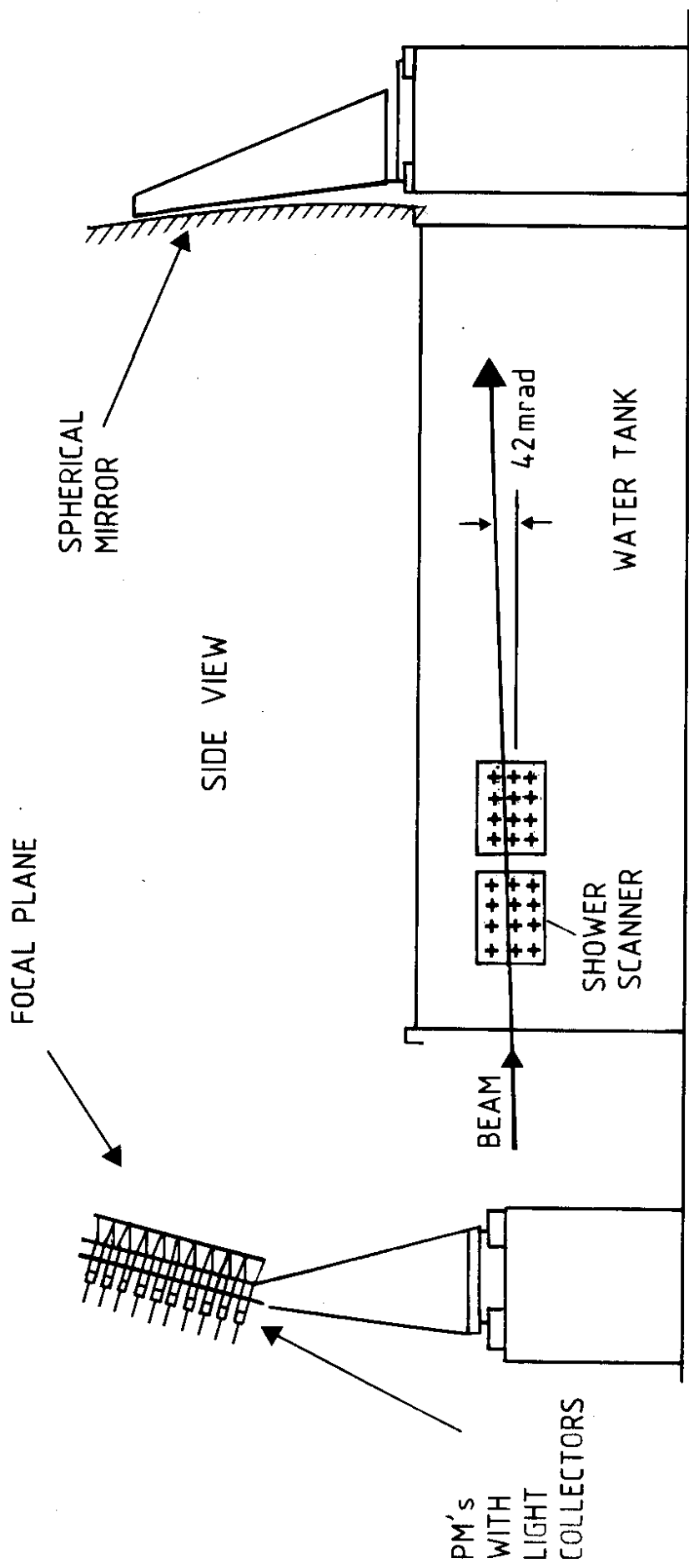


FIG. 2a

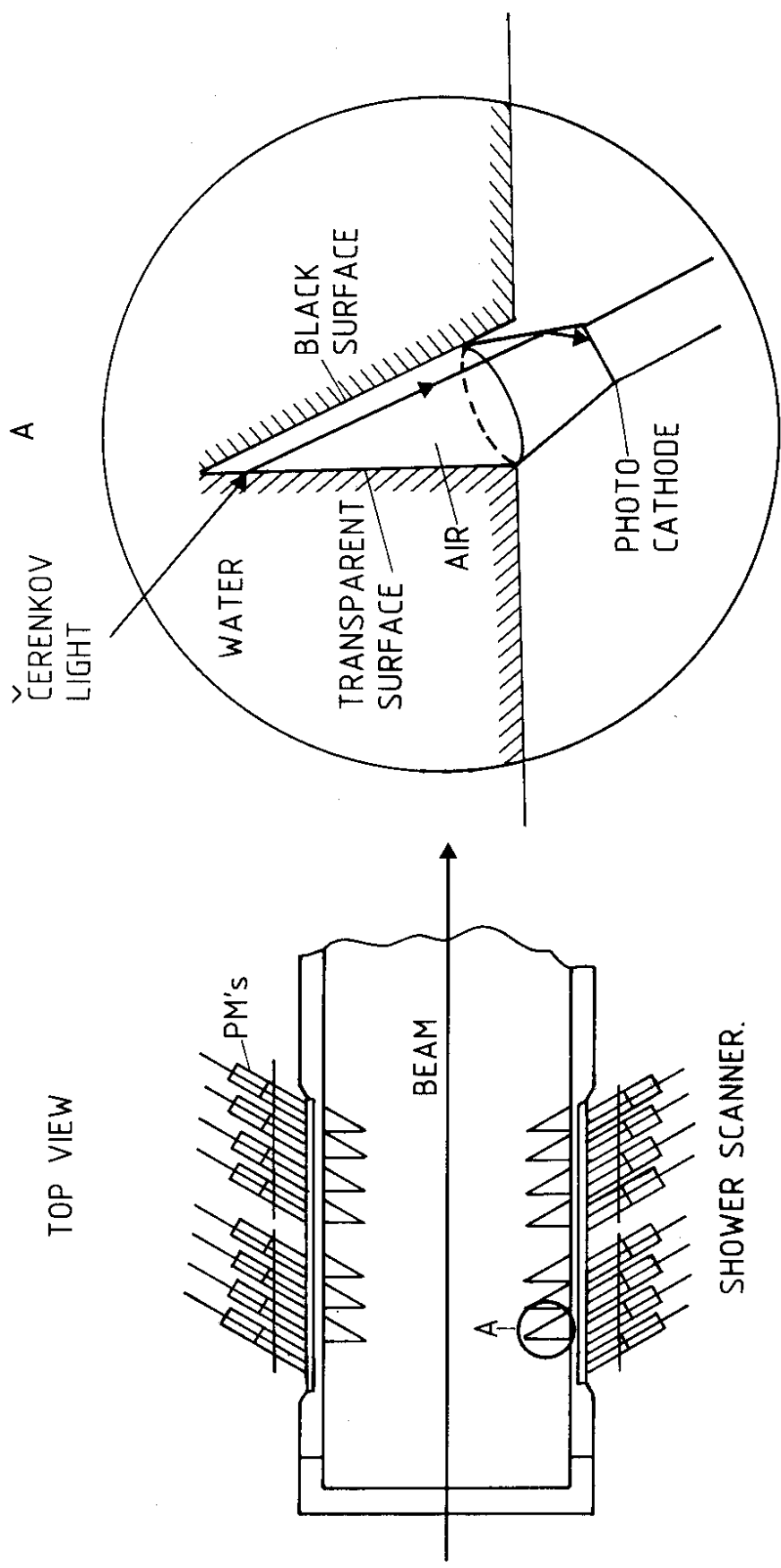


FIG. 2b

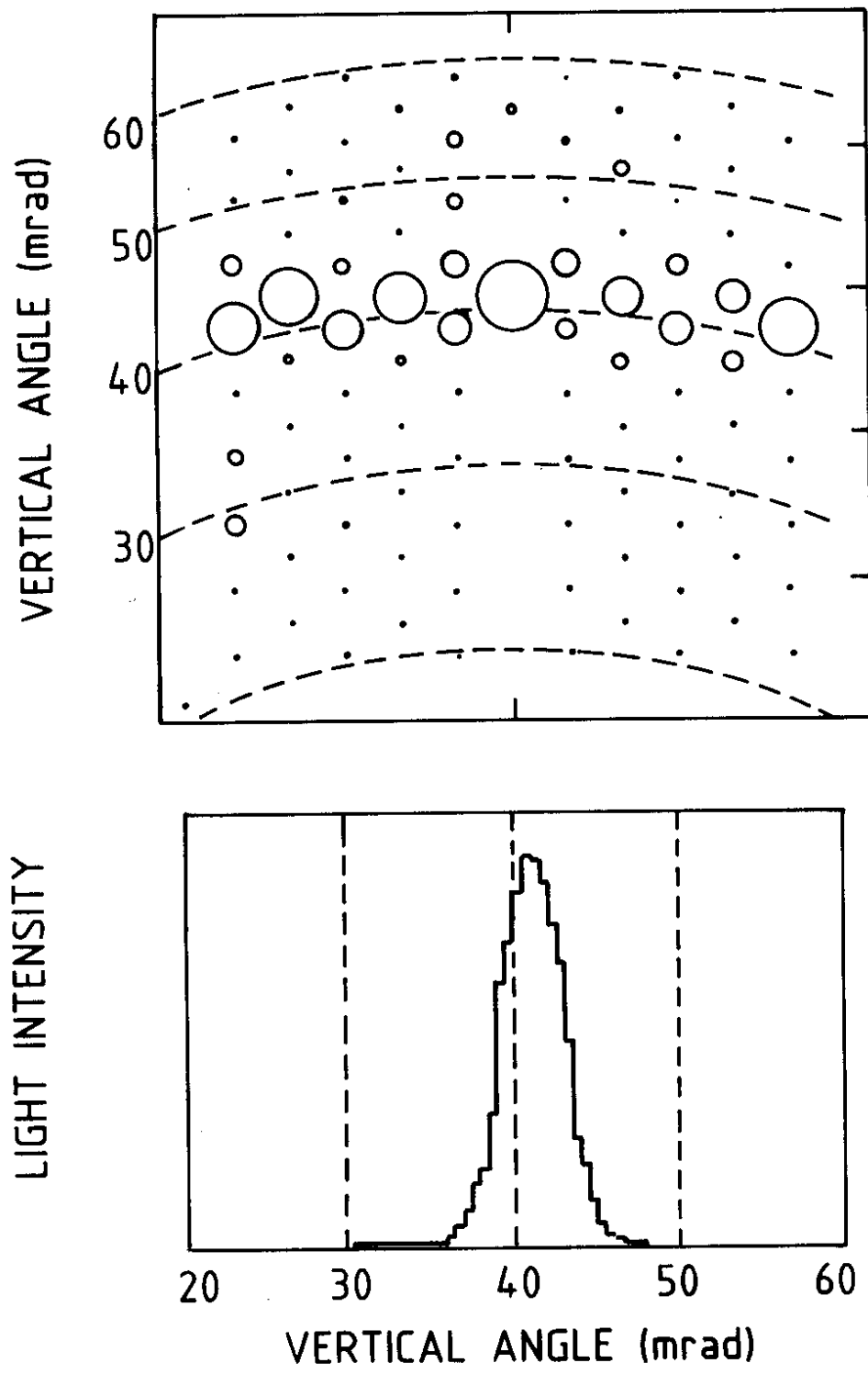


FIG. 3

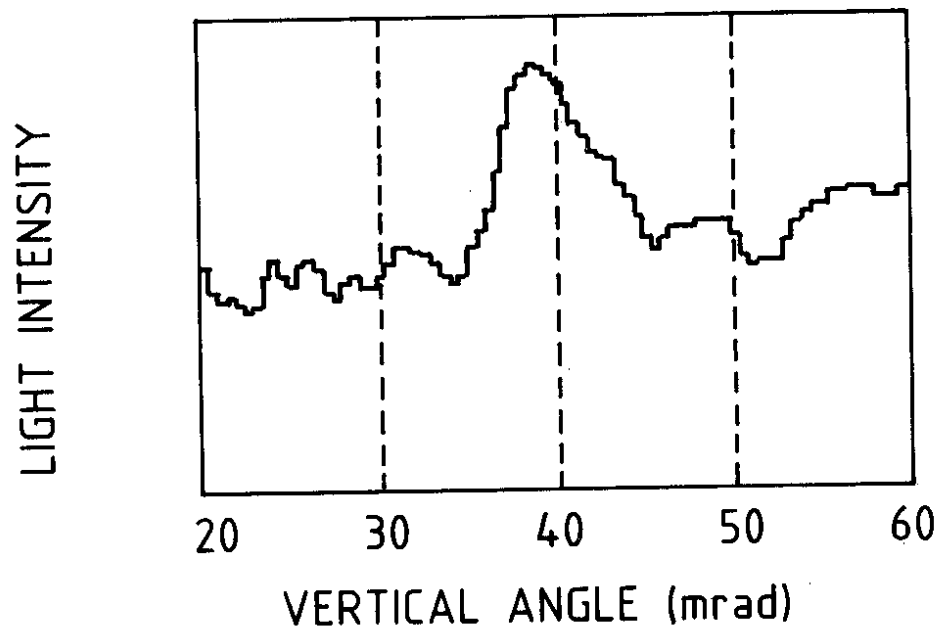
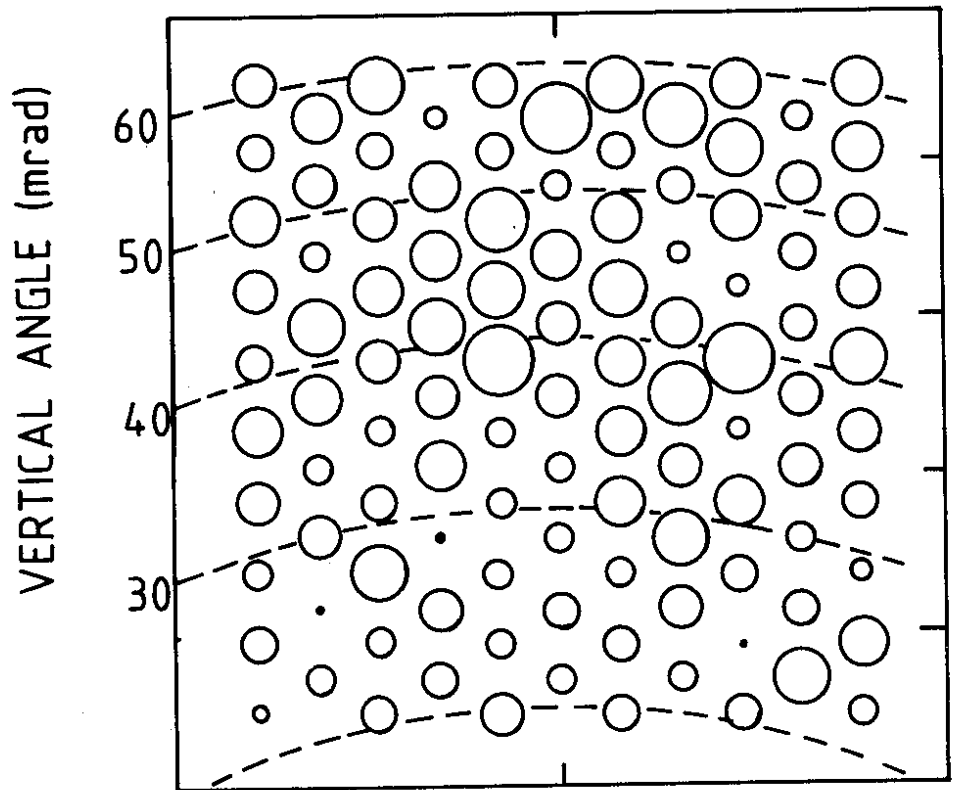


FIG. 4

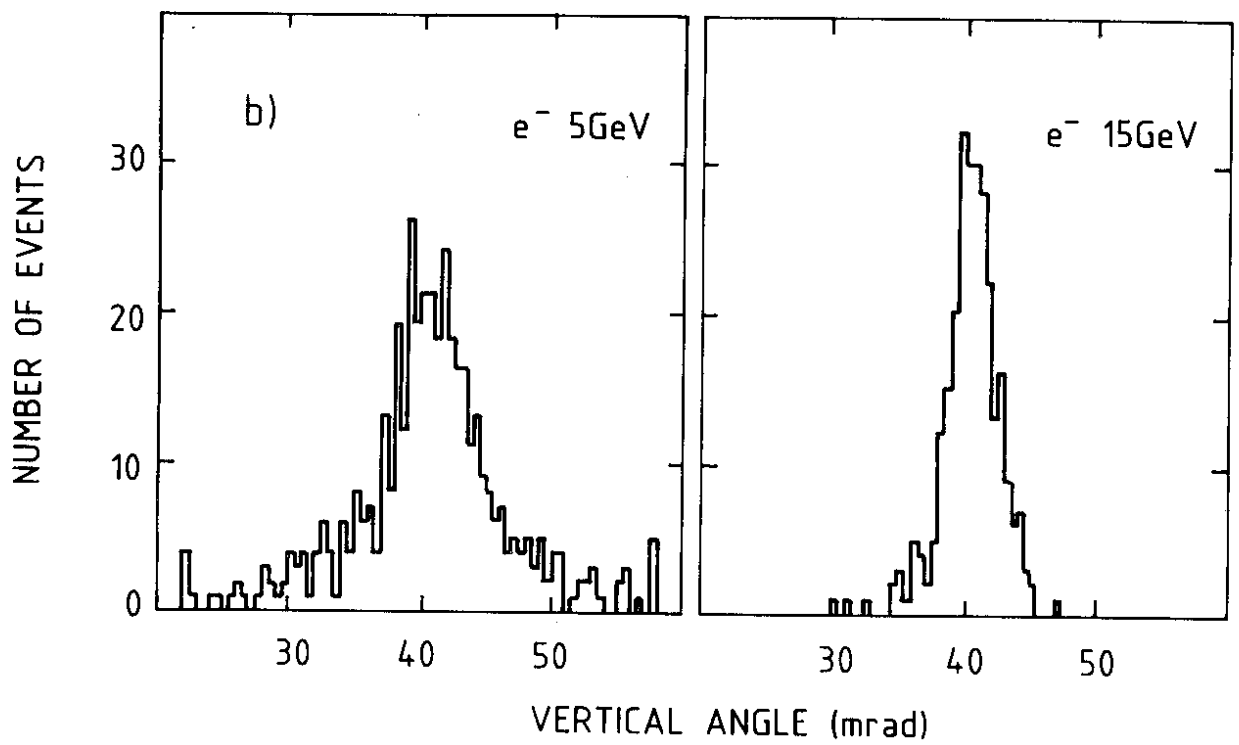
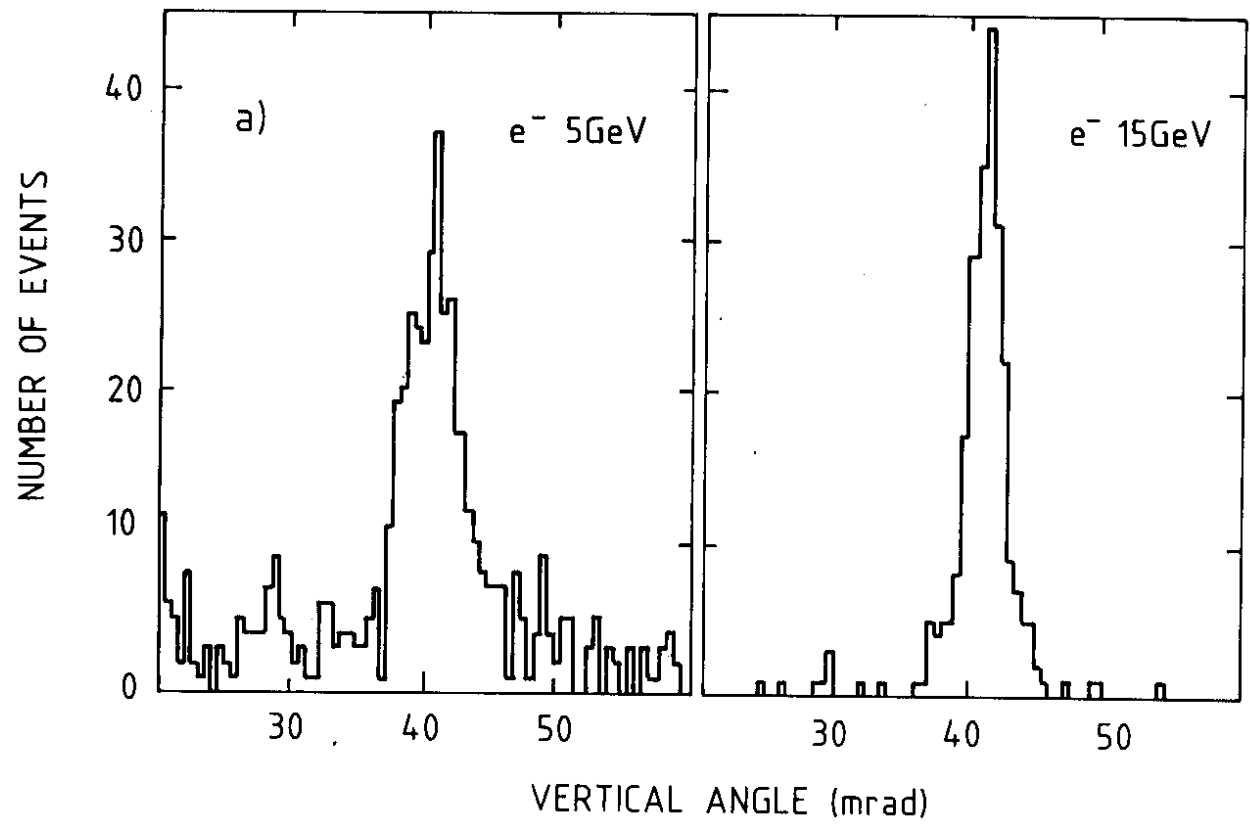


FIG. 5

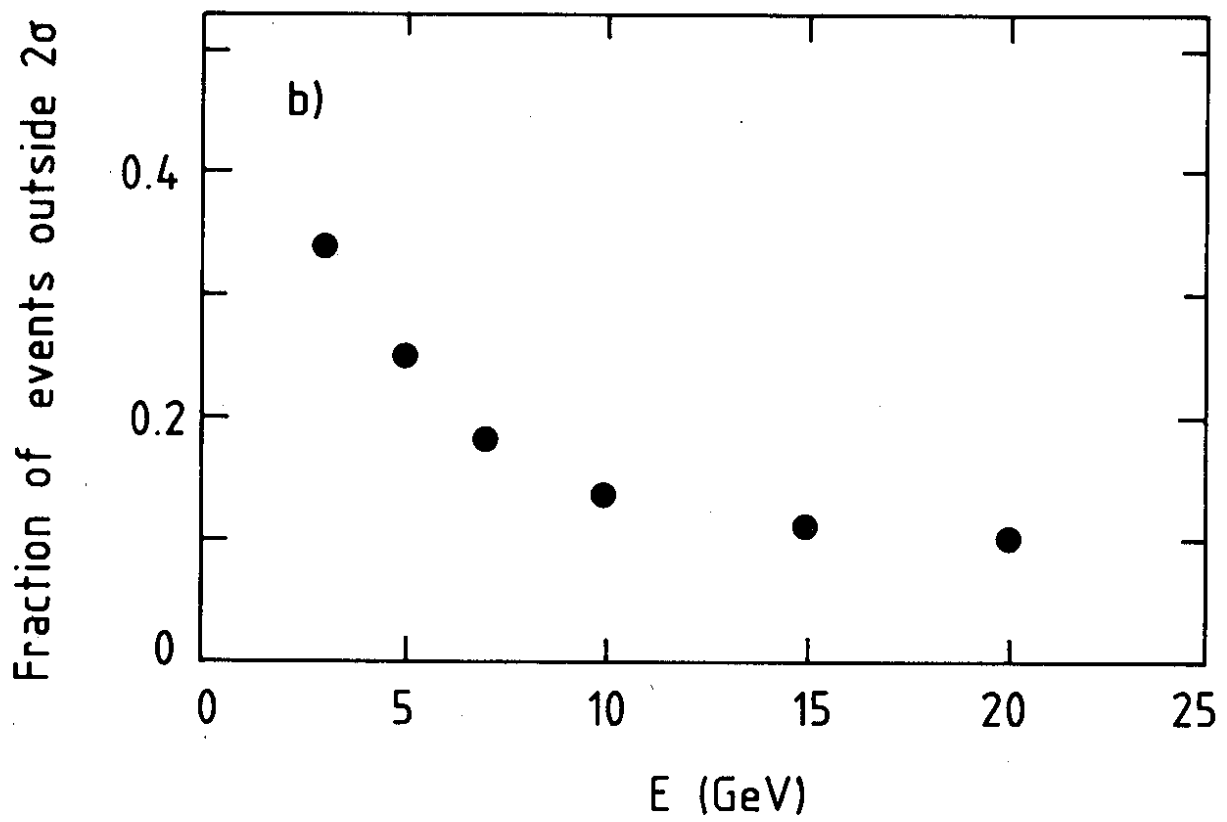
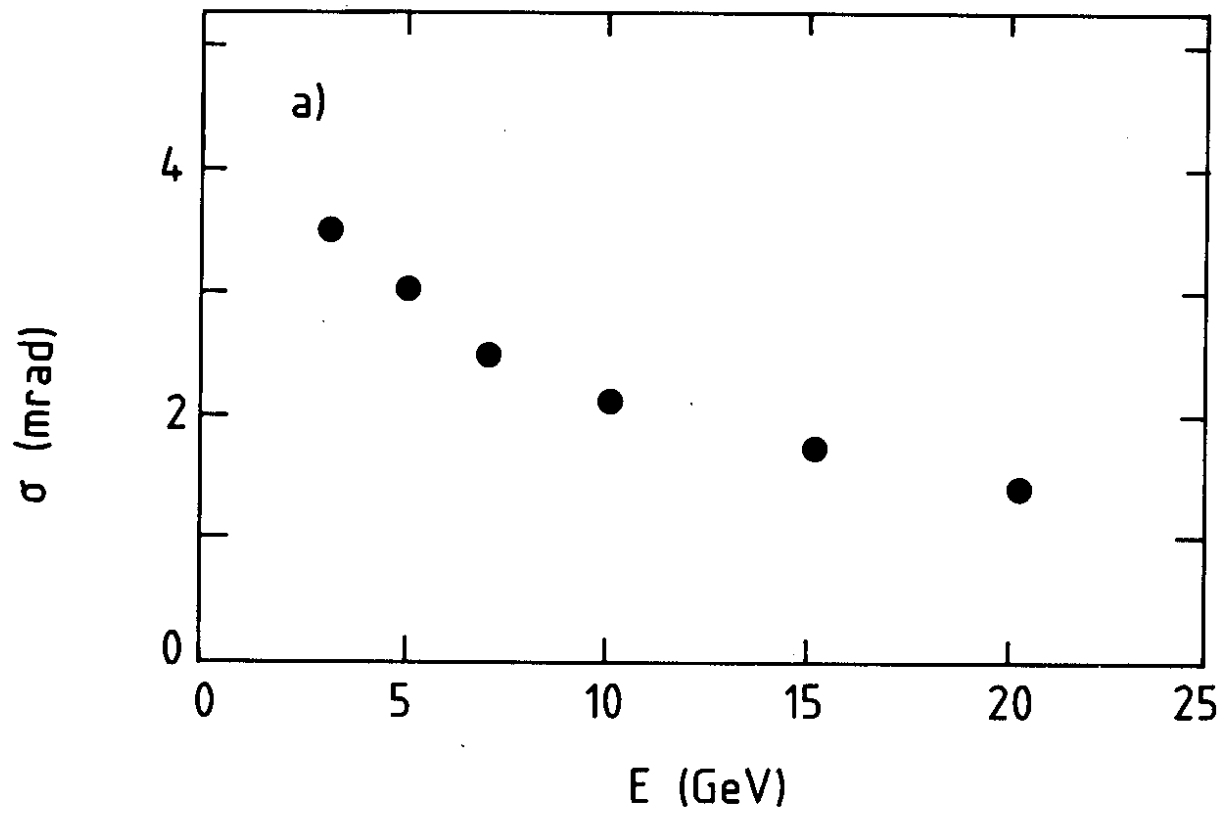


FIG. 6

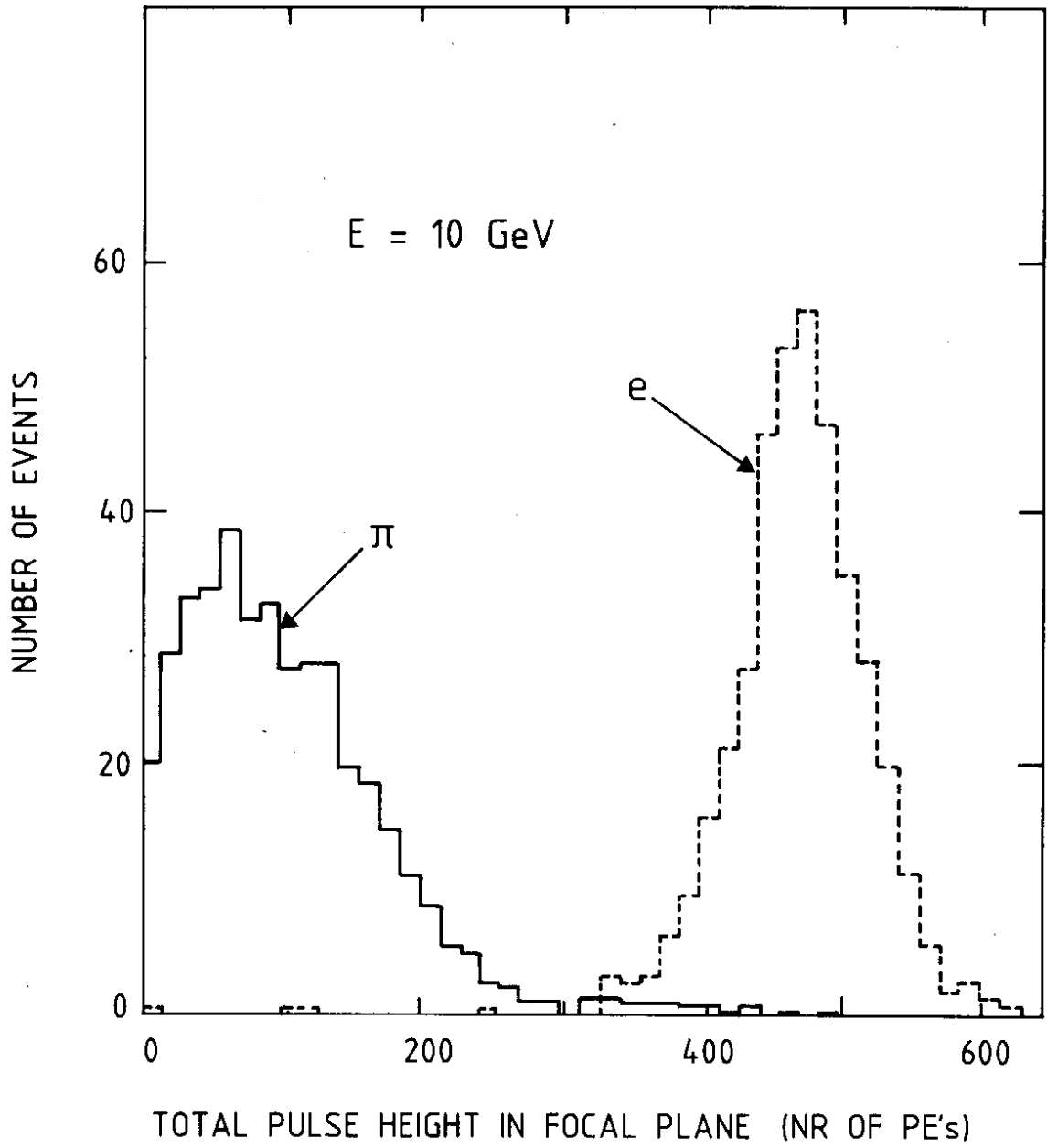
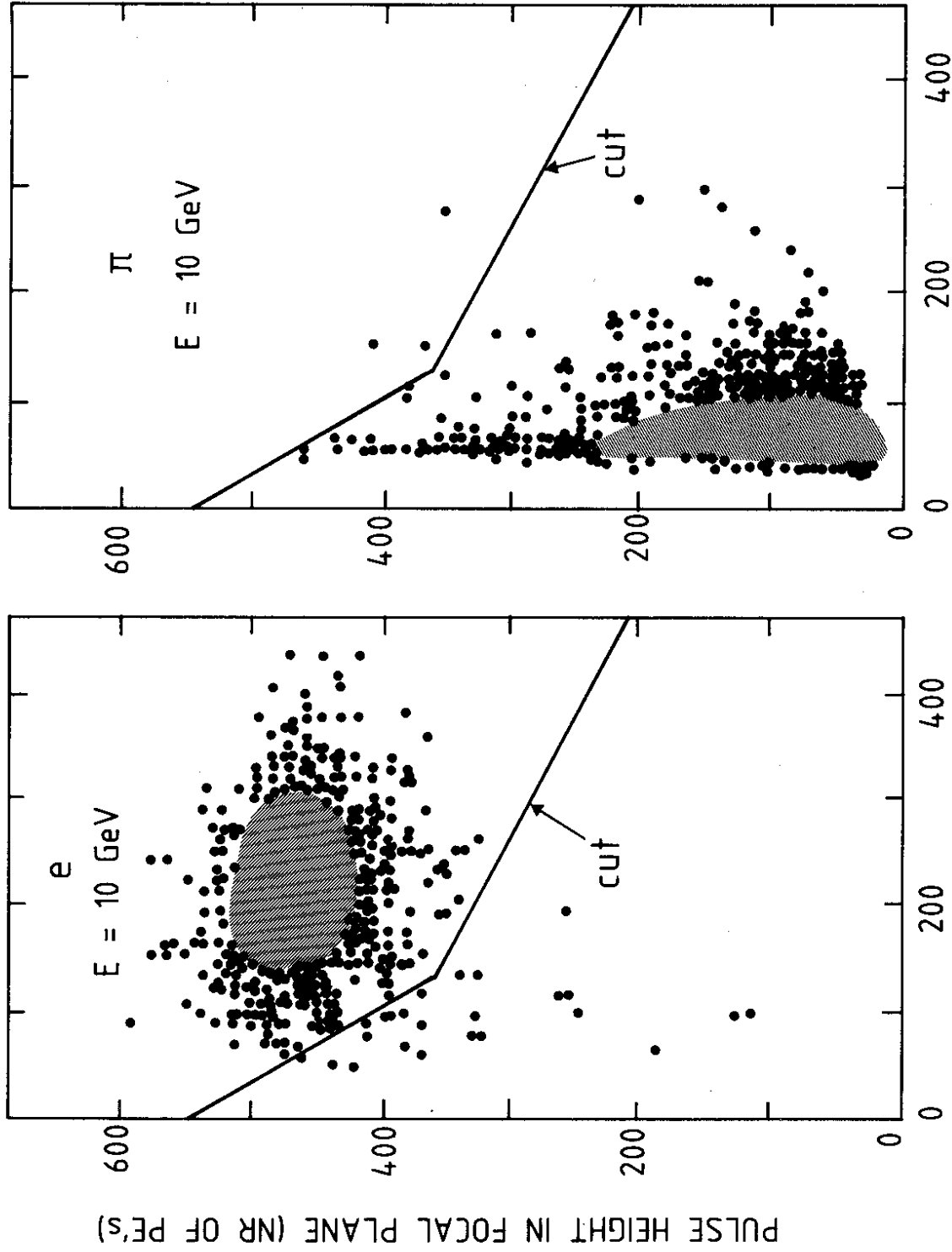


FIG. 7



PULSE HEIGHT IN SHOWER SCANNER (NR OF PE's)

FIG. 8

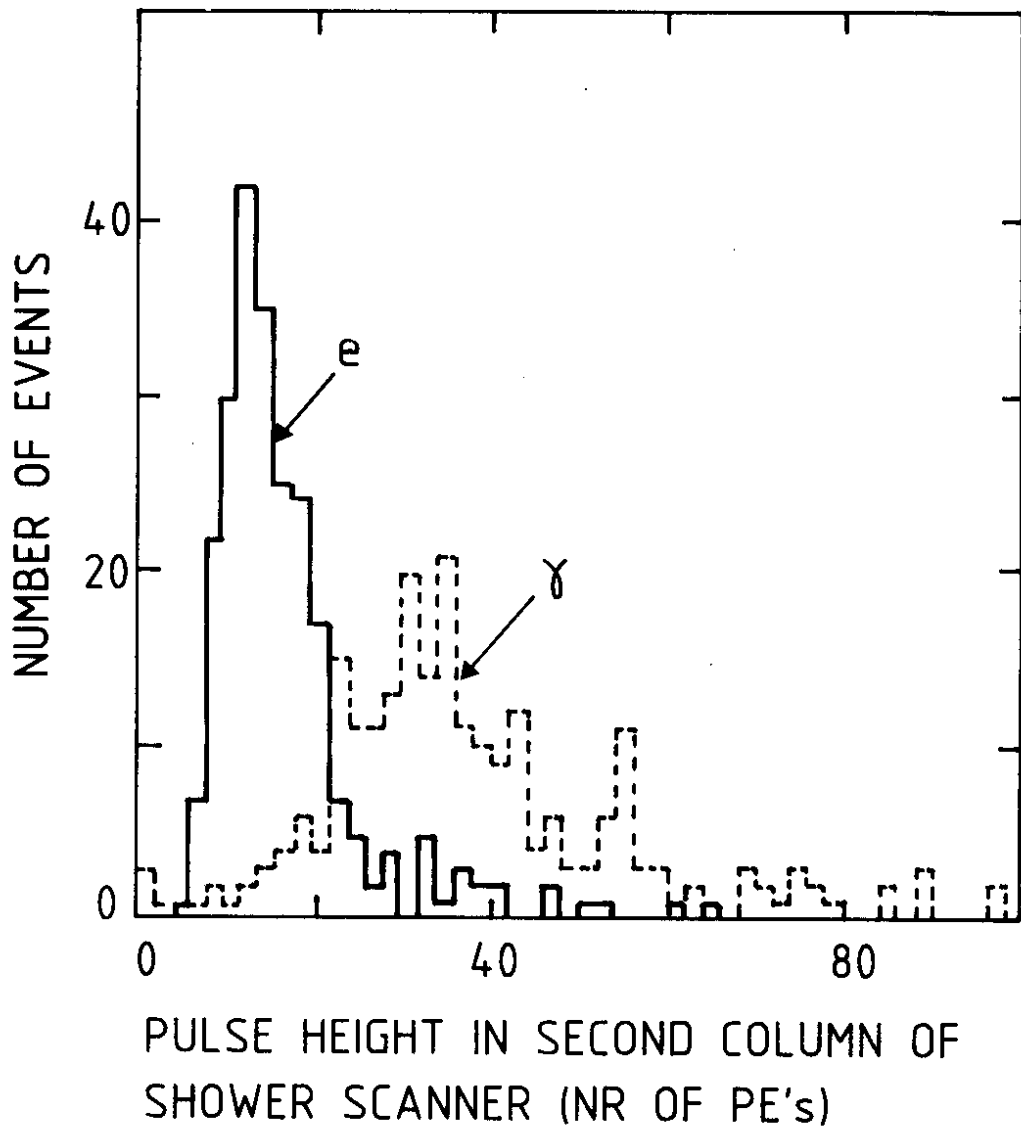


FIG. 9

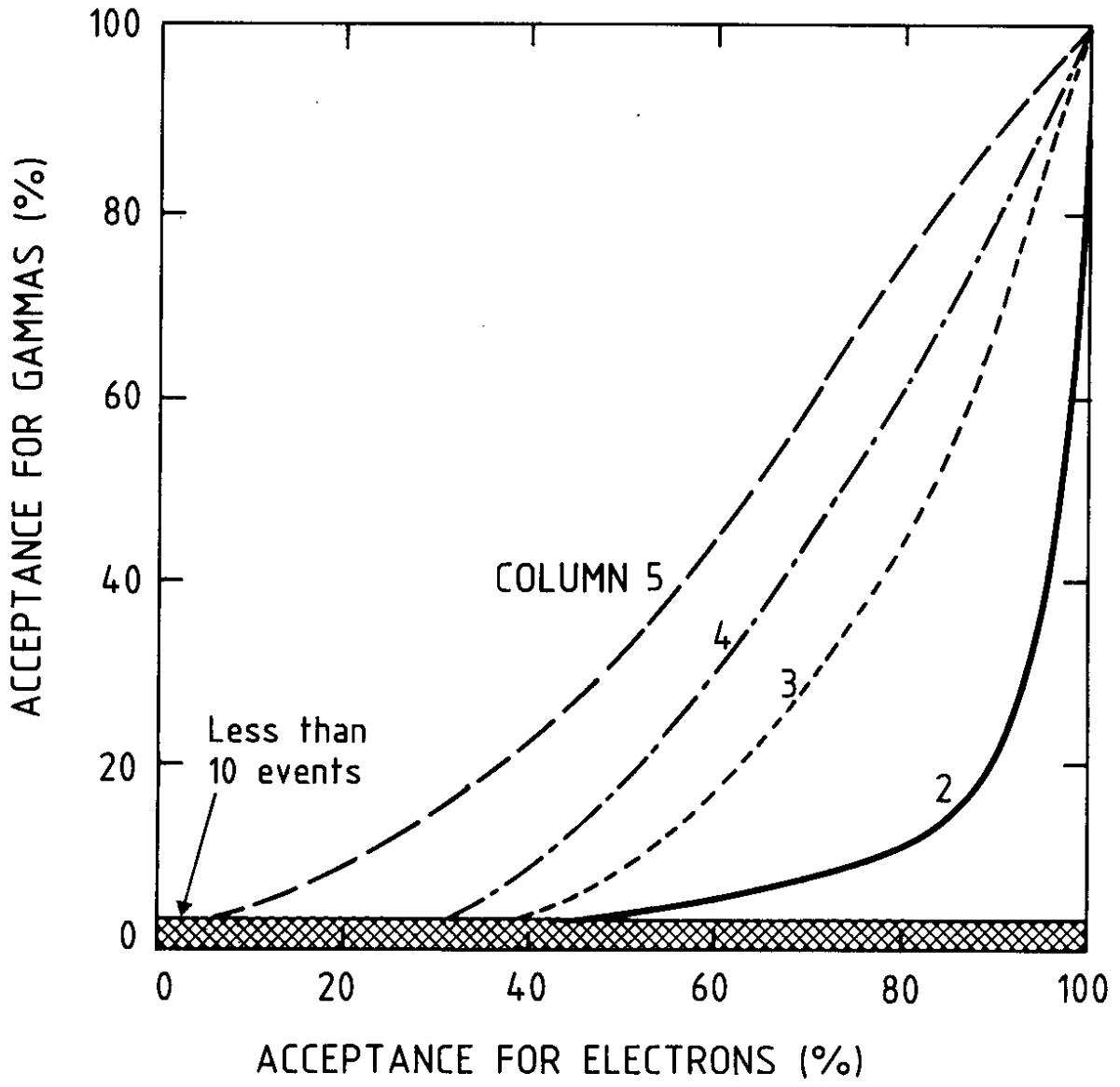


FIG. 10